2020 8th IEEE International Conference on Biomedical
Robotics and Biomechatronics (BioRob)
New York, USA. Nov 29 - Dec 1, 2020

Motion Planning for Active Prosthetic Knees

Mahdy Eslamy, Felix Oswald, Arndt F. Schilling

***Abstract*— A main challenge in the development of active prosthetic knees is how to determine (estimate) the required motion of the missing joint/limb in line with the motion of the remaining biological ones. To do so, a motion planner is required. This study proposes a motion planner for active prosthetic knees. Two inputs (thigh angular velocities and angles obtained from IMU) are used to estimate the corresponding knee joint positions for walking at 0.6, 0.9, 1.2, 1.4 and 1.6 m/s. The motion planner does not require speed estimation, gait percent identification, or switching rules and estimates the outputs (knee joint positions) continuously. This is achieved through a functional ($y = f(x)$) approach. The strengths and limitations of the proposed motion planner are evaluated at different scenarios.**

I. Introduction

To restore transfemoral amputees' locomotion, various active and passive assistive devices have been developed [1]–[13]. Since passive devices are not able to completely emulate the required knee kinematics and kinetics during different speeds and gaits, a great effort has been devoted to develop active devices [7]–[13].

One main challenge in the development of active prosthetic knees is how to determine (estimate) the required motion of the missing joint/limb in line with the motion of the remaining limbs. By doing that, the device can potentially be more supportive to the user. In other words, a motion planner is required so that the actuator in these devices can be triggered in accordance with the locomotion of the user. The output of the motion planner is then the set-point input to the actuator (motor) controller to finally create the required command signal.

Different methods have been developed which can be divided into two main categories. In one approach, the motion planners work based on the division of a gait cycle into four or multiple sections according to the joints' kinematics and kinetics [7]–[9], [11], [12]. These finite-state approaches, then determine the motion of the assistive device at each state (mode) according to the rules defined for each mode. Next, a switching rule(s) is also required which determines when it is required to pass to the next state.

To avoid the efforts required in the former method, some algorithms [10], work based on a continuous procedure which do not require switching rules and dividing a gait cycle into different sections. In [10], the desired knee joint motion was estimated based on the thigh angle and its integral, together with the use of a phase plane. The integral was reset every gait cycle to prevent drift accumulation [10]. Then a set of intermediate parameters were defined to compute a monotonic phase variable. Next, based on the virtual kinematic constraints and discrete Fourier transform, desired knee joint trajectories were estimated. It was reported that controlling the prosthetic device based on the residual thigh motion gave the amputees control over the timing of the prosthetic joints.

Not only different methods have been developed to process the inputs in motion planners, but also different inputs have been used in this regard. The inputs to the motion planners are usually myoelectric EMG signals [14], [15] or mechanical sensors (to measure knee, ankle, foot, shank, thigh kinematics/kinetics) [7], [10]–[12], [16]. For minimizing the complexity and computation, it is preferred to keep the number of the sensory inputs as low as possible [17].

In general, most of the so far developed algorithms work based on the finite-state approach (where a gait cycle is divided into different sections), and very few algorithms work based on a continuous approach [10]. The gait cycle seems to be a continuous process and not a succession of multiple discrete events [18]. Therefore, the state-machine approaches would be less attractive [10], [18] in comparison to the continuous approaches which do not need switching rules and states within a single stride [10].

In this study, the aim was to develop a motion planner for active prosthetic knees that can continuously estimate the knee motion based on the thigh motion. The proposed method does not require speed determination, gait percent identification, or switching rules. Two parameters (thigh angular velocities and angles) were used as inputs to the motion planner. The idea was to take thigh motion as inputs and convert them to knee joint positions as outputs. This is achieved through a function approach, and therefore, a main difference to [10] is that it does not require phase plane approach or defining intermediate parameters to estimate the desired knee positions. This goal is accomplished through Gaussian regression. The proposed method is explained in the next section.

II. Method

A. Fundamentals and Basic Definitions

In Fig. 1, a general control structure for active prosthetic knees is presented. The motion planner (part A) estimates the desired knee positions y in line with the inputs x (thigh angular velocity and angles). The motor controller (part B) (which can be e.g., a PD controller) can then create an error signal $e = y - y_a$ based on the estimated desired value y and the actual value y_a from available sensors. The error

Applied Rehabilitation Technology ART Lab, Department for Trauma Surgery, Orthopaedics and Plastic Surgery, Universitätsmedizin Göttingen (UMG), 37075, Göttingen, Germany, {mahdy.eslamy, arndt.schilling}@med.uni-goettingen.de

978-1-7281-5907-2/20/$31.00 ©2020 IEEE

Authorized licensed use limited to: Technische Universitaet Muenchen. Downloaded on November 27,2023 at 12:36:40 UTC from IEEE Xplore. Restrictions apply.

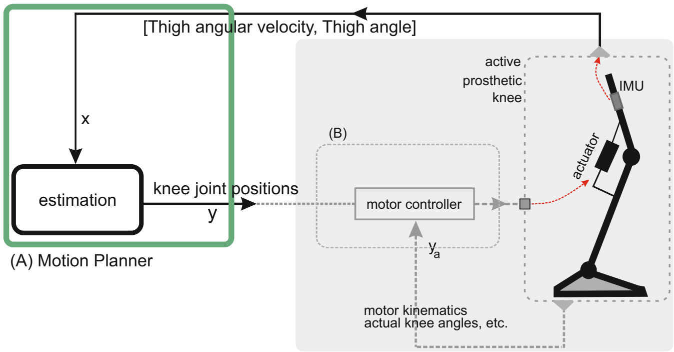

Fig. 1. A general control structure for an active prosthetic knee. The thigh angular velocities and angles are fed into the motion planner (A) to estimate the desired knee joint positions y. In addition, the actual sensory data (y_a) together with y, are used in motor controller (B) to create the required command signal for the actuator (motor). Different actuation mechanisms can be used for an active prosthetic knee [19]. Read section II for detailed information. The focus of this study is on part A.

can then be further processed using gains to finally create an appropriate command signal for the actuator. In this study, the focus is on part A.

According to definition, the gait cycle starts with the heel contact and ends with the next contact of the same foot. A gait cycle is typically divided into one hundred sections called gait percent [20]. Each speed and each gait percent has its corresponding desired joints' and limbs' motions. Basically, the task of the motion planner is to estimate a desired motion for the missing joins/limbs in line with the motions of the remaining joins/limbs. In this study, data of thigh angular velocity $\dot{\theta}_{th}$ and thigh angle θ_{th} were collected for walking 0.6, 0.9, 1.2, 1.4 and 1.6 $\frac{m}{s}$ (healthy male subject, measurement was done through IMU from Xsens MTw Awinda, 100 Hz). The knee joint angles θ_k were obtained by measuring the shank angles and thigh angles and then converting them to the knee angles ($\theta_k = 180 - (\theta_{sh} - \theta_{th})$). The definitions of these angles are schematically shown in Fig. 2.

It should be noted that the motion planner did not require shank data for estimation. The shank data was only required to calculate the corresponding knee angles during walking experiments. These obtained (calculated) knee angles are later compared with the estimated (by the motion planner)

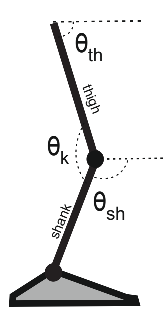

Fig. 2. The definition of knee angle θ_k, thigh angle θ_{th}, and shank angle θ_{sh}.

ones to evaluate the estimation quality and the performance of the motion planner.

As observed in Fig. 1, the thigh angular velocities $\dot{\theta}_{th}$ and thigh angles θ_{th} are the inputs to the motion planner. The knee angles θ_k are the outputs of the motion planner. Both inputs and outputs are divided to training and test groups. The training set is used for learning process, and the testing set is used to evaluate the performance of the motion planner. This point will be explained better later in this section. The motion planner proposed in this study can be used to design high-level controllers for active prosthetic knees whose actuation mechanisms are using a stiff spring [21] or no spring [22], since in these cases, the trajectories of motor positions will be similar to the knee joint positions. The outcome of the estimator can then be used by a motor controller to actuate the prosthesis accordingly. Fully detailed discussions on how to design motor (actuator) trajectories are available in [19], [23]–[25],

B. GP-based Motion Planner

In this study, the problem of designing a motion planner is converted into the problem of finding an appropriate function f that can continuously map the inputs x ($\dot{\theta}_{th}$ and θ_{th}) to the outputs y (knee angles θ_k). This fact can be stated as $y = f(x)$ or equivalently $\theta_k = f(\dot{\theta}_{th}, \theta_{th})$. To define function f, the Gaussian process (GP) regression [26] has been used. Regression in general deals with the prediction of continuous quantities (e.g. in this study knee angles $y = \theta_k$). In fact, the goal is to make inferences about the relationship between the inputs x and the outputs y. The important point is that, the GP Regression aims at learning a function f which can be used to estimate the outputs for the new (unseen) test inputs [26], [27]. Therefore, by training the motion planner, one can evaluate its performance for other untrained situations. That's why we have adopted this approach to design a motion planner.

A GP is defined by its mean $m(x)$ and covariance function $k(x, x')$ (for the input pair x and x') as [26]

$$f(x) \sim \mathcal{GP}(m(x), k(x, x')) \tag{1}$$

where $m(x)$ =E$[f(x)]$ (E denotes expectation of $f(x)$) and $k(x, x')$ =E$[(f(x) - m(x))(f(x') - m(x'))]$. To use GP for prediction, some priori training is required. The training input could be $[\dot{\theta}_{sh}]$ or $[\theta_{sh}]$ or $[\dot{\theta}_{sh}, \theta_{sh}]$ and could be formed like $D = \{(x_i, f_i)|i = 1, \ldots, n\}$. Therefore, it will consist of n observations, where x_i is a d-dimensional input vector and f_i (or in other words y_i) is the corresponding function (output) value (therefore $y_i = f(x_i)$). In addition, concatenating the training observations would form the aggregated input matrix X as

$$X = \begin{pmatrix} x_1 \\ x_2 \\ x_3 \\ \vdots \\ x_n \end{pmatrix}, \quad y = f = \begin{pmatrix} y_1 \\ y_2 \\ y_3 \\ \vdots \\ y_n \end{pmatrix} \tag{2}$$

To evaluate the performance of GP in terms of the estimation (prediction), a test set is also required. The test inputs

Authorized licensed use limited to: Technische Universitaet Muenchen. Downloaded on November 27,2023 at 12:36:40 UTC from IEEE Xplore. Restrictions apply.

are denoted with x^*. Accordingly, the outputs related to x^* are marked with f^* (or in fact $y^* = f^*(x^*)$).

Since the output is continuous and bounded, it is logical to think that inputs close to each other would have quite similar output values and therefore the training inputs that are close to the test inputs should be logically informative for prediction. In GP, the covariance function k defines such a similarity. The covariance function is also a designer-defined parameter. For GP, it is possible to select different functions [26], [27]. In this study we evaluated different functions, in which optimal performance was observed through using Matérn covariance function. The Matérn class of covariance function is in the form of

$$k_{Mat\acute{e}rn}(r) = \frac{2^{1-\nu}}{\Gamma(\nu)}(\frac{\sqrt{2\nu}r}{l})^{\nu}K_{\nu}(\frac{\sqrt{2\nu}r}{l}) \tag{3}$$

r is the the absolute difference of input pairs x and x' ($r = |x - x'|$), ν and l are positive parameters called hyper-parameters Θ, where K_ν is a modified Bessel function [26]. One common approach to determine the hyperparameters is to maximize the log marginal likelihood [26], [27]

$$logp(y|X,\Theta) = -\frac{1}{2}(y^T K(X,X)y + log|K(X,X)| + nlog2\pi) \tag{4}$$

in which $p(A|B)$ means conditional probability of A given that event B is true. The first term of Eq. 4 addresses data fit, the second term introduces a complexity penalty and the last term is a normalization constant. The log marginal likelihood automatically performs a trade-off between model fit and complexity. Several optimization algorithms could be used. In this study hyperparameters were optimized by different approaches, and optimal performance was observed when exact inference method together with Gaussian Likelihood was used.

The joint distribution of the training outputs f and the test outputs f^* would be [26]

$$\begin{bmatrix} f \\ f^* \end{bmatrix} \sim \mathcal{N}\left(0, \begin{bmatrix} K(X,X) & K(X,X^*) \\ K(X^*,X) & K(X^*,X^*) \end{bmatrix}\right) \tag{5}$$

where $K(X,X^*)$ is the $n \times n^*$ matrix of the covariances evaluated at all pairs of training and test points. A $K(X,X)$ is defined as

$$K(X,X) = \begin{pmatrix} k(x_1,x_1) & k(x_1,x_2) & \cdots & k(x_1,x_n) \\ k(x_2,x_1) & k(x_2,x_2) & \cdots & k(x_2,x_n) \\ \vdots & \vdots & \vdots & \vdots \\ k(x_n,x_1) & k(x_n,x_2) & \cdots & k(x_n,x_n) \end{pmatrix} \tag{6}$$

A similar statement could be expected for other $K(.,.)$. $\mathcal{N}$ denotes normal distribution.

In light of Eq. 5, it is possible to obtain information for f^* on the condition of having X, f and X^* as

$$f^*|X, f, X^* \sim \mathcal{N}(\bar{f}^*, cov(f^*)), \text{ where} \tag{7a}$$

$$\bar{f}^* = K(X^*,X)K(X,X)^{-1}f \tag{7b}$$

$$\text{cov}(f^*) = K(X^*,X^*) - K(X^*,X)K(X,X)^{-1}K(X,X^*) \tag{7c}$$

where $\bar{f}^*$ and $\text{cov}(f^*)$ are GP posterior mean and GP posterior covariance respectively. Eqs. 7 provide the solution for f^* to estimate (predict) the desired outputs related to the unseen new test inputs (i.e. the test inputs X^*). Consequently, this method shows the potentials that can be used as a candidate for developing motion planners for active prosthetic knees.

To evaluate the estimation quality of the motion planner different scenarios are devised. In the following scenarios, the estimated values of knee angles are compared with the previously obtained knee angles.

To fulfill the comparison task, the root-mean-square (RMS) errors, mean absolute deviations (MADs), maximum absolute errors and the commonly used R^2 values are compared between different scenarios. These measures were employed in different studies, e.g., [28]–[30].

A literature survey shows that there is no defined gold criterion to determine which estimation results should be deemed acceptable and not acceptable for active prosthetics. Nevertheless, the same criterion that was used in [30] was also used in this study to determine acceptable estimation quality. In that study, R^2 values higher than 0.8 were a sign of acceptable estimations (the maximum is 1). However, there are some studies in which the experimental R^2 values are less than the above-mentioned threshold, [31], but the experiments were apparently conducted with satisfactory user performance.

In scenario 1, the thigh angular velocities and thigh angles of two gait cycles are used for training (for 0.6, 0.9, 1.2, 1.4 and 1.6 m/s). Then, the estimation quality (i.e. the estimation of the knee angles) is evaluated for another thirteen gait cycles (for those same speeds).

In scenario 2, the leave-one-out cross validation is used to evaluate the estimation quality which is a common approach for this purpose [14], [32]–[34]. In this scenario, the thigh angular velocities and thigh angles of two gait cycles for four speeds are used for training. Next, the estimation quality is evaluated for thirteen gait cycles of the untrained fifth speed. This procedure is done for all of those five speeds individually.

In scenario 3, the interpolation capability of the motion planner is evaluated. To do this, the thigh angular velocities and thigh angles of two gait cycles for 0.6 and 1.6 m/s are used for training. Afterwards, the estimation quality is evaluated for thirteen gait cycles of 0.9, 1.2 and 1.4 m/s.

In scenario 4, the extrapolation capability of the motion planner is evaluated. To do this, the thigh angular velocities and thigh angles of two gait cycles for 0.6 and 0.9 m/s are used for training. Afterwards, the estimation quality is evaluated for thirteen gait cycles of 1.2, 1.4 and 1.6 m/s. The obtained results are discussed in the following section.

III. Results

In Fig. 3 the results of the root mean square (RMS) errors, mean absolute deviations (MADs), maximum absolute errors

Authorized licensed use limited to: Technische Universitaet Muenchen. Downloaded on November 27,2023 at 12:36:40 UTC from IEEE Xplore. Restrictions apply.

and R^2 values are comparatively shown for those four scenarios and five speeds under investigation.

According to the above-mentioned acceptance criterion, the best performance is related to the first scenario, i.e., the case that the motion planner was trained for all of the speeds and was tested by new unseen inputs but from the same speeds. In this case, the corresponding R^2 values are the highest (except for 1.2 m/s, which is slightly less than scenario 3 for this speed).

In general, the R^2 values are above the acceptance threshold (0.8). However, in scenario 2, for 0.6 m/s the value is less than the success threshold (about 5% difference). As observed, the R^2 values for interpolation study (scenario 3) are higher than the values for extrapolation study (scenario 4). This can show that the method of training can play a role for the success level of the motion planner (for instance, compare the values for 1.2 and 1.4 m/s). However, still, in both cases the values are above the acceptance threshold. With regard to R^2 values, in general, the lowest values are seen for scenario 4 (extrapolation study).

The mean RMS errors are comparable to the results reported in [35]. The mean values of maximum absolute errors are within the range seen in [10], [35]. The R^2 values are also in the range reported by [28]. However, it should be noted that this study used only two types of inputs.

To better visualize the estimated knee joint positions in comparison to the measured ones, in Fig. 4, the curves are shown for five gait cycles for those five speeds (curves related to scenario 1).

IV. Discussions & Conclusions

As observed, the best performance was related to scenario 1. However, in other scenarios, the acceptance criterion was met as well. This can show that the motion planner performed acceptably for various scenarios. Furthermore, the estimations were done using few sensory inputs and in addition, the motion planner performed continuously without being required to design switching rules.

Apart form these advantages, it is also important to have the limitations of the proposed motion planner in mind. For instance, the motion planner should also be evaluated for other gaits such as ascending and descending the stairs or slopes. Moreover, the transition between gaits should also be investigated, for example, when the user wants to stand up and start walking. These issues can form the frame for future studies. Furthermore, the results were investigated for one male subject. To have more robust conclusions about the performance of the motion planner, more experiments with different subjects are required.

Another point that requires more studies is how to determine a success criterion. For instance, looking at different studies, it is seen that variations between the planned trajecto-

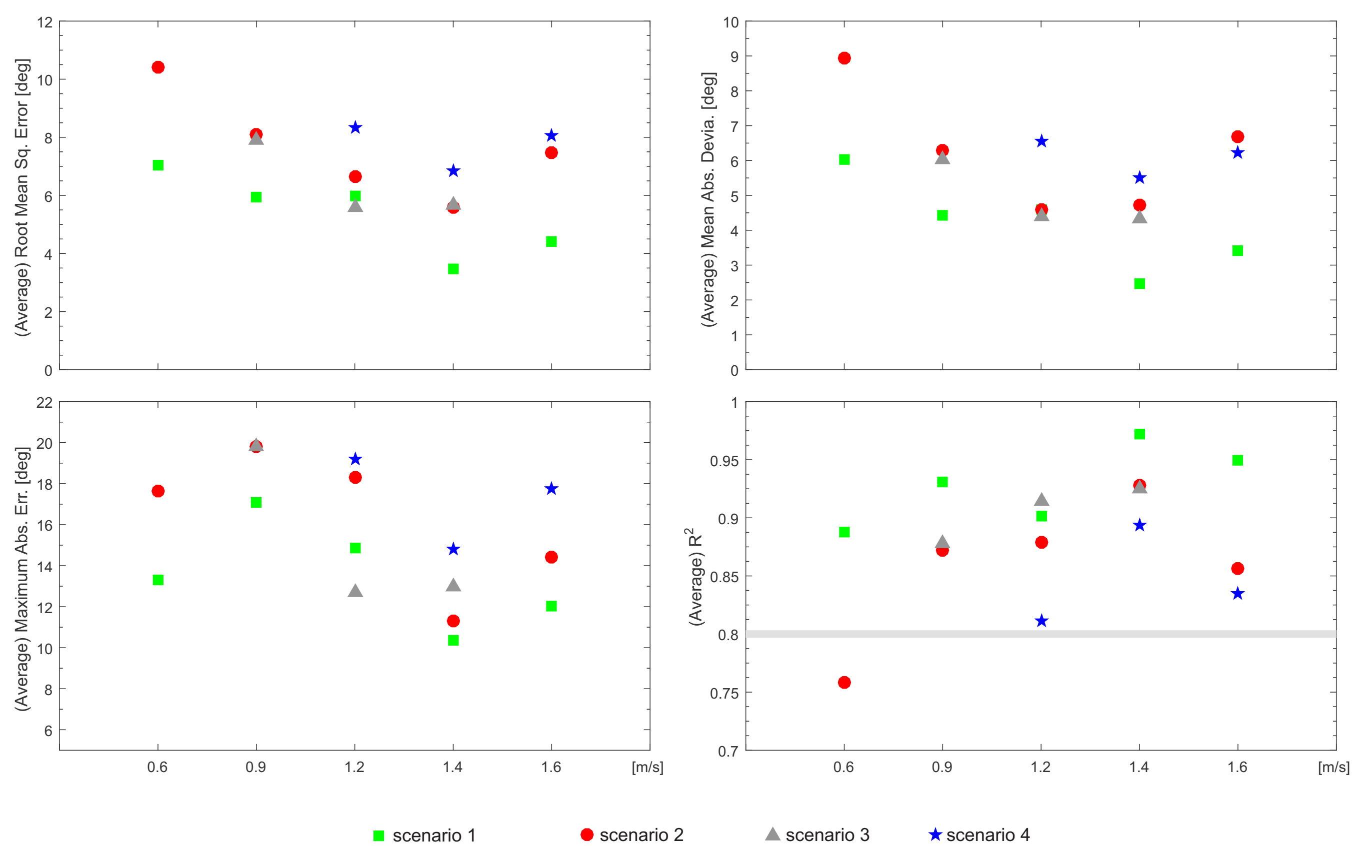

Fig. 3. The comparison (of the average values of thirteen gait cycles) of root mean square (RMS) errors, mean absolute deviations (MAD), maximum absolute errors and R^2 values between those four scenarios explained in Methods section (for 0.6, 0.9, 1.2, 1.4, and 1.6 m/s).

Authorized licensed use limited to: Technische Universitaet Muenchen. Downloaded on November 27,2023 at 12:36:40 UTC from IEEE Xplore. Restrictions apply.

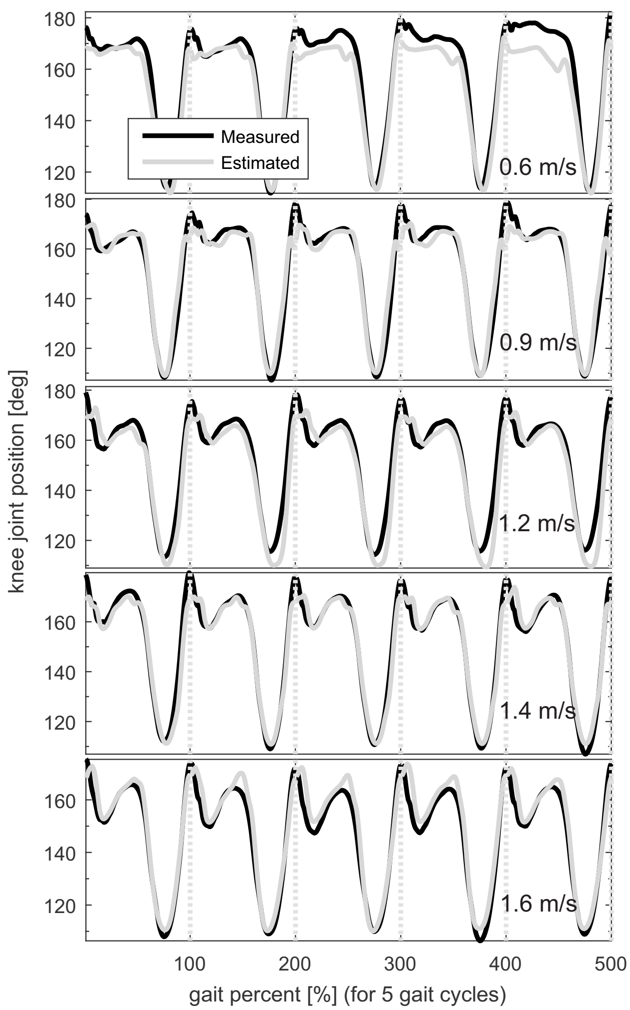

Fig. 4. The comparison between the measured and the estimated knee joint positions for 0.6, 0.9, 1.2, 1.4, and 1.6 m/s for five gait cycles, (results related to scenario 1, see Results for more details).

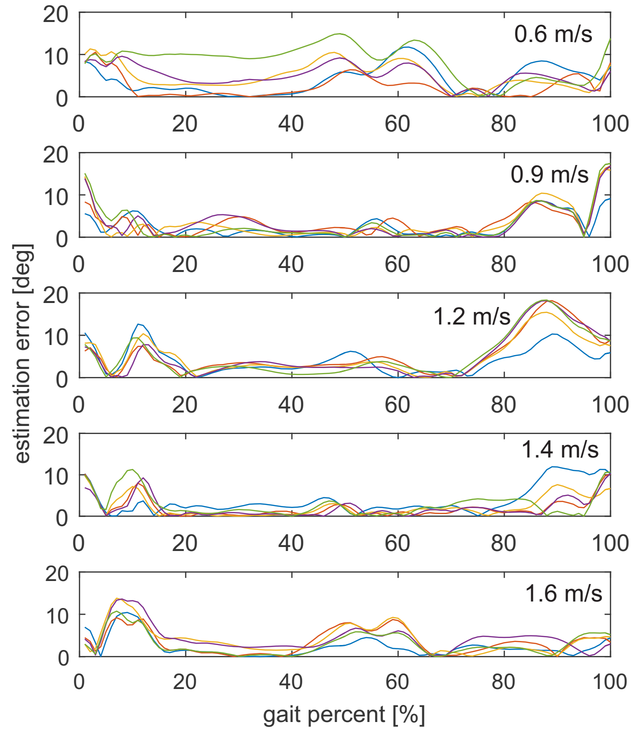

Fig. 5. The comparison of the estimation errors between five gait cycles at each speed (related to scenario 1).

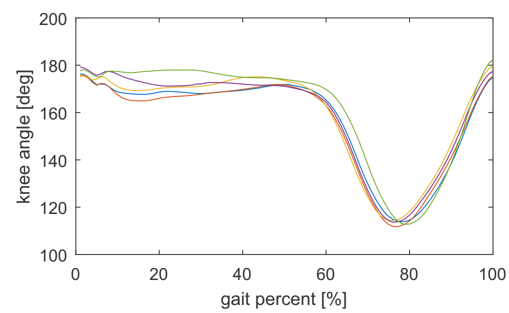

Fig. 6. The comparison of the measured knee joint positions between five gait cycles, curves for 0.6 m/s.

ries and the obtained trajectories are visible e.g., [10], [31], [36], [37], but apparently the experiments were done with user satisfaction or at least no severe impact on the user was observed during those experiments. This matter makes it even more challenging to define how exactly knee joint trajectories should be estimated (and consequently emulated by an assistive device). Therefore, a more comprehensive criterion that can provide a better tool to evaluate the quality of the estimations, seems necessary. This might necessitate taking different parameters into attention, for instance kinematics, kinetics and muscular activities (EMG signals). However, on the other side, it may be challenging how to develop a success criterion while taking into account those different variables.

In addition, as observed in Fig. 3, the motion planner had the best performance when it received a full training (i.e., the training and testing speeds were the same). The reason that for other scenarios the performance was lower than scenario 1, may not only be due to the algorithm. The results might potentially get better if multiple inputs were used. For instance if more kinematics data or EMG data were included simultaneously. It was shown in [32] that sensor fusion approach (EMG + mechanical) can result in better prosthesis control compared to the methods that use only EMG signals or only mechanical sensors. This issue can be investigated more in the future to evaluate if the performance can be improved according to the above hypothesis.

To investigate if the estimation errors have occurred in special sections of the gait cycles, the errors have been shown for those five speeds (scenario 1) in Fig. 5. As seen, the distribution of the estimation errors are more or less different not only between the speeds but also between the gait cycles of a single speed. Another important matter that should be taken into account is that the human gait is a dynamic phenomenon, and therefore, to expect that the joint trajectories are the same amongst the gait cycles, does not

Authorized licensed use limited to: Technische Universitaet Muenchen. Downloaded on November 27,2023 at 12:36:40 UTC from IEEE Xplore. Restrictions apply.

hold. This fact has been shown in Fig. 6 for gait cycles at 0.6 m/s. As observed, there are variations between the knee joint trajectories even for a single speed and for a single person. Therefore, it poses even more challenges in front of a motion planner to estimate the joint trajectories perfectly well during locomotion.

The success of any algorithm needs to be investigated in clinical experiments. By this way, the limitations and the strengths of the motion planning algorithm can be identified much better. To do so, the next step is to evaluate this algorithm in assistive devices in the future.

V. Acknowledgement

The required data for this work was obtained from Applied Rehabilitation Technology Laboratory, Universitätsmedizin Göttingen (UMG), Germany. This work was supported by the Grant from the Bundesministerium für Bildung und Forschung (BMBF) (INOPRO-16SV7656).

References

[1] [Online]. Available: https://www.ossur.com/prosthetic-solutions/products/all-products/knees-and-legs/mauch-knee

[2] [Online]. Available: http://www.ottobockus.com/C-Leg.html

[3] [Online]. Available: https://www.ossur.com/prosthetic-solutions/products/dynamic-solutions/rheo-knee-3

[4] [Online]. Available: https://www.ossur.com/prosthetic-solutions/products/dynamic-solutions/power-knee

[5] D. Grimes, W. Flowers, and M. Donath, "Feasibility of an active control scheme for above knee prostheses," *Journal of Biomechanical Engineering*, vol. 99, no. 4, pp. 215–221, 1977.

[6] D. L. Grimes, "An active multi-mode above knee prosthesis controller," Ph.D. dissertation, Massachusetts Institute of Technology, 1979.

[7] F. Sup, A. Bohara, and M. Goldfarb, "Design and control of a powered transfemoral prosthesis," *The International Journal of Robotics Research*, vol. 27, no. 2, pp. 263–273, 2008.

[8] B. E. Lawson, H. A. Varol, A. Huff, E. Erdemir, and M. Goldfarb, "Control of stair ascent and descent with a powered transfemoral prosthesis," *IEEE Transactions on Neural Systems and Rehabilitation Engineering*, vol. 21, no. 3, pp. 466–473, 2013.

[9] E. J. Rouse, L. M. Mooney, and H. M. Herr, "Clutchable series-elastic actuator: Implications for prosthetic knee design," *The International Journal of Robotics Research*, vol. 33, no. 13, pp. 1611–1625, 2014.

[10] D. Quintero, D. J. Villarreal, D. J. Lambert, S. Kapp, and R. D. Gregg, "Continuous-phase control of a powered knee–ankle prosthesis: Amputee experiments across speeds and inclines," *IEEE Transactions on Robotics*, pp. 686–701, 2018.

[11] H. Varol, F. Sup, and M. Goldfarb, "Real-time gait mode intent recognition of a powered knee and ankle prosthesis for standing and walking," in *IEEE RAS & EMBS International Conference on Biomedical Robotics and Biomechatronics (BioRob)*, 2009, pp. 66–72.

[12] H. Varol, F. Sup, and M. Goldfarb, "Multiclass real-time intent recognition of a powered lower limb prosthesis," *IEEE Transactions on Biomedical Engineering*, vol. 57, no. 3, pp. 542–551, 2010.

[13] A. Kilicarslan, S. Prasad, R. G. Grossman, and J. L. Contreras-Vidal, "High accuracy decoding of user intentions using eeg to control a lower-body exoskeleton," in *International conference of the IEEE Engineering in medicine and biology society (EMBC)*, 2013, pp. 5606–5609.

[14] H. Huang, T. Kuiken, and R. Lipschutz, "A strategy for identifying locomotion modes using surface electromyography," *IEEE Transactions on Biomedical Engineering*, vol. 56, pp. 65–73, 2009.

[15] D. Jin, J. Yang, R. Zhang, R. Wang, and J. Zhang, "Terrain identification for prosthetic knees based on electromyographic signal features," *Tsinghua Science & Technology*, vol. 11, no. 1, pp. 74–79, 2006.

[16] H. Varol, F. Sup, and M. Goldfarb, "Powered sit-to-stand and assistive stand-to-sit framework for a powered transfemoral prosthesis," in *IEEE International Conference on Rehabilitation Robotics (ICORR)*, 2009, pp. 645–651.

[17] H. L. Bartlett and M. Goldfarb, "A phase variable approach for imu-based locomotion activity recognition," *IEEE Transactions on Biomedical Engineering*, vol. 65, no. 6, pp. 1330–1338, 2018.

[18] D. J. Villarreal, H. A. Poonawala, and R. D. Gregg, "A robust parameterization of human gait patterns across phase-shifting perturbations," *IEEE Transactions on Neural Systems and Rehabilitation Engineering*, vol. 25, no. 3, pp. 265–278, 2017.

[19] P. Scholl, V. Grabosch, M. Eslamy, and A. Seyfarth, "Comparison of peak power and energy requirements in different actuation concepts for active knee prosthesis," in *IEEE International Conference on Mechatronics and Automation*, 2015, pp. 1448–1453.

[20] M. W. Whittle, *Gait analysis: an introduction*, 2003.

[21] M. Grimmer and A. Seyfarth, "Stiffness adjustment of a series elastic actuator in a knee prosthesis for walking and running: The trade-off between energy and peak power optimization," in *IEEE International Conference on Intelligent Robots and Systems (IROS)*, 2011, pp. 1811–1816.

[22] F. Sup, H. A. Varol, J. Mitchell, T. Withrow, and M. Goldfarb, "Design and control of an active electrical knee and ankle prosthesis," in *IEEE RAS & EMBS International Conference on Biomedical Robotics and Biomechatronics (BioRob)*, 2008, pp. 523–528.

[23] M. Grimmer, M. Eslamy, S. Gliech, and A. Seyfarth, "A comparison of parallel- and series elastic elements in an actuator for mimicking human ankle joint in walking and running," in *IEEE International Conference on Robotics and Automation (ICRA)*, 2012, pp. 2463–2470.

[24] M. Eslamy, M. Grimmer, and A. Seyfarth, "Effects of unidirectional parallel springs on required peak power and energy in powered prosthetic ankles: Comparison between different active actuation concepts," *IEEE Internationall Conference on Robotics and Biomimetics*, pp. 2406–2412, 2012.

[25] M. Eslamy, M. Grimmer, S. Rinderknecht, and A. Seyfarth, "Does it pay to have a damper in a powered ankle prosthesis? a power-energy perspective," *IEEE International Conference on Rehabilitation Robotics (ICORR)*, pp. 1–8, 2013.

[26] C. E. Rasmussen and C. K. I. Williams, *Gaussian Processes for Machine Learning*. The MIT Press, 2006.

[27] [Online]. Available: http://www.gaussianprocess.org/gpml

[28] A. Findlow, J. Goulermas, C. Nester, D. Howard, and L. Kenney, "Predicting lower limb joint kinematics using wearable motion sensors," *Gait & posture*, vol. 28, no. 1, pp. 120–126, 2008.

[29] J. Goulermas, D. Howard, C. Nester, R. Jones, and L. Ren, "Regression techniques for the prediction of lower limb kinematics," *Journal of Biomechanical Engineering*, vol. 127, no. 6, pp. 1020–1024, 2005.

[30] R. A. Bogey and L. A. Barnes, "An EMG-to-force processing approach for estimating in vivo hip muscle forces in normal human walking," *IEEE Transactions on Neural Systems and Rehabilitation Engineering*, vol. 25, no. 8, pp. 1172–1179, 2017.

[31] N. Dhir, H. Dallali, E. M. Ficanha, G. A. Ribeiro, and M. Rastgaar, "Locomotion envelopes for adaptive control of powered ankle prostheses," in *IEEE International Conference on Robotics and Automation (ICRA)*, 2018, pp. 1488–1495.

[32] H. Huang, F. Zhang, L. J. Hargrove, Z. Dou, D. R. Rogers, and K. B. Englehart, "Continuous locomotion-mode identification for prosthetic legs based on neuromuscular–mechanical fusion," *IEEE Transactions on Biomedical Engineering*, vol. 58, no. 10, pp. 286–2875, 2011.

[33] A. J. Young, A. M. Simon, N. P. Fey, and L. J. Hargrove, "Intent recognition in a powered lower limb prosthesis using time history information," *Annals of Biomedical Engineering*, vol. 42, no. 3, pp. 631–641, 2014.

[34] A. J. Young, A. M. Simon, and L. J. Hargrove, "A training method for locomotion mode prediction using powered lower limb prostheses," *IEEE Transactions on Neural Systems and Rehabilitation Engineering*, vol. 22, no. 3, pp. 671–677, 2013.

[35] R. Takeda, S. Tadano, A. Natorigawa, M. Todoh, and S. Yoshinari, "Gait posture estimation using wearable acceleration and gyro sensors," *Journal of biomechanics*, vol. 42, no. 15, pp. 2486–2494, 2009.

[36] A. H. Shultz, J. E. Mitchell, D. Truex, B. E. Lawson, E. Ledoux, and M. Goldfarb, "A walking controller for a powered ankle prosthesis," in *IEEE Engineering in Medicine and Biology Society Conference*. IEEE, 2014, pp. 6203–6206.

[37] M. Tran, L. Gabert, M. Cempini, and T. Lenzi, "A lightweight, efficient fully powered knee prosthesis with actively variable transmission," *IEEE Robotics and Automation Letters*, vol. 4, no. 2, pp. 1186–1193, 2019.

Authorized licensed use limited to: Technische Universitaet Muenchen. Downloaded on November 27,2023 at 12:36:40 UTC from IEEE Xplore. Restrictions apply.